

Using Hilbert Curves to Organize, Sample, and Sonify Solar Data

W. Dean Pesnell¹ and Kyle Ingram-Johnson²

¹ *NASA Goddard Space Flight Center, Greenbelt, MD, USA* and*

² *Eleanor Roosevelt High School, Greenbelt, MD, USA*

Abstract

How many ways can we explore the Sun? We have images in many wavelengths and squiggly lines of many parameters that we can use to characterize the Sun. We know that while the Sun is blindingly bright to the naked eye it has regions that are dark in some wavelengths of light it is bright in others. But both of those classifications are based on vision. Hearing is another sense that can be used to explore solar data. Some data, such as the sunspot number or the extreme ultraviolet spectral irradiance, can be readily sonified. Images are more difficult. A simple raster scan of a full-disk image of the Sun is dominated by the pattern of moving on and off the limb of the Sun. Any sonification of the raster scan will contain discontinuities at the limbs that mask the information contained in the image. Hilbert curves are continuous space-filling curves that map a linear variable onto the two-dimensional coordinates of an image. We have investigated using Hilbert curves as ways to sample and analyze solar images. Reading the image along a Hilbert curve keeps most neighborhoods close together as the resolution (i.e., the order of the Hilbert curve) increases. It also removes most of the detector size periodicities and may reveal longer-scale features. We provide several examples of sonified solar data, including the sunspot number, a selection of extreme ultraviolet (EUV) spectral irradiances, different ways to sonify an EUV image, and a series of EUV images during a filament eruption.

21 I. INTRODUCTION

22 Sonifying a data set has the basic purpose of adding another dimension to the data or making
23 the data accessible to the blind. Helping all to visualize a data set in a new way is another goal.
24 Musical concepts such as pitch, duration, loudness, timbre, and pan will be described and used to
25 sonify data. Rhythms are simplified to assigning the distance between points as the beat, and we do
26 not try for a harmonic composition, instead concentrating on timbres to build the sonic structure.
27 By identifying the rhythm of the music with the pulse of the physical data we are neither producing
28 *Musique concrète* nor would our sonifications be considered traditional music.

29 Composers have used many ways to create sounds and music that mimic the natural and me-
30 chanical worlds. Camille Saint-Saëns used pianos and other instruments to imitate about 14 an-
31 imals in *The Carnival of the Animals*. Old-time fiddle tunes use the flexibility of the combined
32 performer and violin to imitate chickens and other natural sounds. Luigi Russolo built “intonaru-
33 mori” to produce a broad spectrum of modulated, rhythmic sounds that imitated machines.¹ He
34 also developed a graphical form of musical score to compose pieces for these devices. Others
35 have produced music from time sequences of the natural world. A well-known example is *Concret*
36 *PH*,² which was created by splicing together short, random segments of tape recordings of burning
37 charcoal.

38 Analog electronic synthesizers were the next step. In their early stages they were often used to
39 produce sound effects. As analog synthesizers became more capable, such as the Moog machines,
40 some used them to reproduce well-known musical pieces in electronic form (e.g., *Switched-On*
41 *Bach* by Wendy Carlos, 1968) while others invented new types of music (the improvisations of
42 Keith Emerson in the works of Emerson, Lake, and Palmer.)

43 Few, if any, of these techniques are examples of sonifying data. Sonification can be as simple
44 as the shrieking of a smoke alarm or as complicated as converting multi-dimensional data to an
45 audible signal. The incessant beeps and whistles of electronic vital sign monitors in hospitals are
46 one example where the change in a sound signals a change in health of the patient. These use the
47 1-D structure of sound to convey information that conditions are both normal and alarming.

48 Digital electronic synthesizers give us the ability to convert any type of information from a dig-
49 ital representation into music.³ A 1-D time series can be sonified by scaling the values into musical

50 pitches, assuming a constant duration for each value, and producing a set of MIDI commands. A
51 MIDI synthesizer is then used to create the musical instrument waveforms and play the commands
52 in the MIDI file. Different time series can be combined into a sonification by using different pitch
53 ranges or timbres to distinguish between them. We will use the International Sunspot Number
54 (Version 2, S) and extreme ultraviolet (EUV) spectral irradiances from two satellites as examples
55 of solar time series data.

56 Sonifying an image is different. Sound is intrinsically a 1-D format that evolves in time. A 2-D
57 image must be converted to a 1-D series of pixel values where the order of the pixels serves as the
58 time variable. Once the 1-D sequence exists, the pixel values are scaled to pitches, the duration is
59 again set to a constant, and the data run through the synthesizer.

60 There are many ways to map a 2-D image (or higher-dimensioned data) to a 1-D sequence. A
61 raster scan is a linear reading of the image from the upper left to the lower right moving down to
62 the next row when the current one is read, much like reading an English language document. This
63 can be modified into a boustrophedonic algorithm where the first row is read left to right and the
64 next right to left, continuing in this way to the end of the image. This resembles the way an ox
65 plows a field and hence the name as *bous* is Greek for ox. Other methods use Z-order curves to
66 map higher-dimensioned data onto a 1-D sequence. Morton⁴ describes using Z-order curves to
67 access a file address database. Another way is to use a space-filling curve, such as the Hilbert used
68 here, to map the image pixels to a sequence. We will describe using Hilbert curves to convert 2-D
69 images into 1-D sequences and converting those sequences to sound.

70 Sonifications of these data sets will be described:

- 71 1. International Sunspot Number (annual and monthly variations)
- 72 2. Extreme ultraviolet (EUV) spectral irradiances as a time series and spectrum
- 73 3. A complete EUV image and seven subimages
- 74 4. Montage of EUV images showing a filament liftoff

75 All of the sound files are available as .midi and .mp3 files at [https://sdo.gsfc.nasa.gov/sonify/
76 table.html](https://sdo.gsfc.nasa.gov/sonify/table.html).

77 We start by introducing some useful musical concepts. That will be followed by a discussion of
78 the synthesizer used and the analysis of of the 1-D data sets. The image data will be introduced and

79 an example using a raster scan to convert the data to 1-D will be described. We will then describe
 80 the Hilbert curves used to address the image data and present several ways to address the images.
 81 We discuss what can be learned from these sonifications and end with several conclusions on the
 82 utility of this method. All of the science datasets are open-source and are available at the locations
 83 listed in the Acknowledgements.

84 II. SONIFYING DATA

85 The JythonMusic software described in Manaris and Brown⁵ was used to convert a data series
 86 into MIDI commands and drive a synthesizer. That means the concepts and terms we use to convert
 87 data to music are:

- 88 • **Pitch:** One of 128 frequencies (spanning 10.75 octaves, from 8.18 Hz [C_{-1}] – 12.54 kHz
 89 [G_9]), with Middle C (C4, 261.63 Hz) roughly in the middle at position 60. Twenty one
 90 pitches are added below the lowest note on the piano and 19 pitches above the highest note. A
 91 range of only 128 values is small compared to the linear range of many solar and geophysical
 92 data sets. It is also small compared to the pitch discrimination of human ears. Untrained
 93 humans can discern pitch changes of $\gtrsim 1\%$, so at least 12800 pitches would be necessary to
 94 resolve that frequency range. However, the MIDI standard allows limited microtones at that
 95 spacing. JPEG images have pixel values ranging from 0–255 (either in separate channels or
 96 through a color table), so we have only half of the range in pitches. Transforming the data
 97 into logarithms also reduces the range from orders of magnitude to small enough to sonify.
- 98 • **Duration:** The lengths of pitches and rests (periods of time without any sound) are specified
 99 with a floating point number that can vary from 0 (no time) to 4 (corresponds to a whole note)
 100 and longer. They are relative to the tempo of the piece, increasing the tempo proportionally
 101 reduces the duration of all pitches and rests. Tempo is specified by the number of beats per
 102 minute (bpm), where a quarter note (QN in JythonMusic) is one beat.
- 103 • **Loudness:** The loudness (also called the dynamics or MIDI velocity) is set by an integer in
 104 the range 0 (silent) to 127 (very, very loud). As the range of sound pressure level varies from
 105 0 dB (threshold of hearing) to 120 dB (threshold of pain), the loudness maps to a change

106 of roughly one per dB. The response of human ears to loudness variations strongly varies
107 from one person to another and with frequency. The least noticeable change in loudness also
108 varies with frequency, but a reasonable value is 0.4 dB.⁶ This corresponds to a 5% change in
109 pressure and is easily accommodated by the 128 possible values. We only use loudness to
110 weight the various datasets. It is also possible to encode information in the loudness, such
111 as a longer duration being louder, but we do not present such cases here.

- 112 • **Timbre:** There are 128 possible voices in the MIDI standard. These timbres are not specified
113 in the MIDI standard and a numbered timbre may sound different in different synthesizers.
114 One channel is devoted to percussion and uses the pitch designator to select a percussive
115 timbre.
- 116 • **Pan:** Position in space is limited in this study to left-right pan. A floating point number
117 between 0 (left) and 1 (right) determines the position, with 0.5 (centered) the default. Placing
118 one data set in the left side and another in the right is a good way to compare two data sets.
119 Where they agree the sounds will appear to come from the middle and otherwise they will
120 come from separate sides.

121 JythonMusic is based on Java rather than C. Programs in JythonMusic are written in Python
122 2.7 syntax but do not have access to many of the libraries used for numerical work. Data access
123 and extraction routines were written and executed in either a C-based Python environment or the
124 IDL language. The provides access to the NumPy library for array manipulation while the latter
125 can handle the scientific data file formats. The computational sequence was to read the data,
126 extract the appropriate part, write the extracted data to a CSV file, read that file in the JythonMusic
127 environment, convert the data into a MIDI file, and use the synthesizer to play that file.

128 **III. SAMPLING AND SONIFYING SOLAR DATA**

129 Several types of solar data were sonified and reported here. A summary is presented in Table I,
130 where the source, type, and name of MP3 file are listed. The Sec. column is the part of the paper
131 where the data is described. A version of this table, with links to the MP3 and MIDI files, is
132 available at <https://sdo.gsfc.nasa.gov/sonify/table.html>.

TABLE I. Files for each Sonified Data Set

Sec.	Source	Sonified Data	mp3 Filename
III A	SIDC	Sunspot number	TS_sunspot_annual_month.mp3
III B	SEE	EUV spectral irradiances	TS_SEE_sonified.mp3
III B	EVE	EUV spectral irradiances	TS_EVE_sonified.mp3
III C	AIA 193 Å	Complete image (raster)	AIA_193_full_image_sonified_raster.mp3
V	AIA 193 Å	Complete image (Hilbert)	AIA_193_full_image_sonified.mp3
V A	AIA 193 Å	Subimage 1 (Arcs)	subimage_1_x_685_y_1755.mp3
V A	AIA 193 Å	Subimage 2 (Fan)	subimage_2_x_1060_y_1120.mp3
V A	AIA 193 Å	Subimage 3 (Island)	subimage_3_x_1290_y_1690.mp3
V A	AIA 193 Å	Subimage 4 (Limb)	subimage_4_x_1800_y_992.mp3
V A	AIA 193 Å	Subimage 5 (Spot)	subimage_5_x_890_y_1035.mp3
V A	AIA 193 Å	Subimage 6 (Swirl)	subimage_6_x_750_y_1125.mp3
V A	AIA 193 Å	Subimage 7 (X)	subimage_7_x_760_y_405.mp3
V B	AIA 193 Å	Filament liftoff montage	liftoff_complete.mp3

134 A. International Sunspot Number

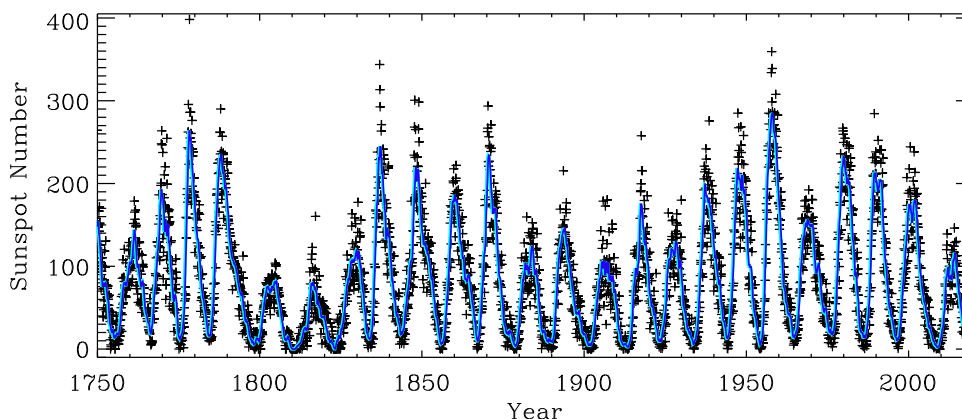
135 The first example is the variation of the International Sunspot Number (S) with time. The
136 sunspot number is a weighted count of dark regions on the Sun that is often used as a long-term
137 index of solar activity. It has been measured or derived for roughly 400 years. It is the source of
138 much of our knowledge of the evolution of solar activity. We use Version 2 of the International
139 Sunspot Number^{7,8} between 1749 Jan 01 and 2018 Dec 31 from the Solar Influences Data analysis
140 Center (SIDC) website, both the monthly and annual averages. The time dependence of S is shown
141 in Figure 1.

142 The lower voice (PICKED_BASS timbre) is used for the annually-averaged data, which also
143 determines the beat. The high voice (PIANO timbre) is used for the monthly average, which plays
144 at 12 values per beat, and was panned left-right with a two-year period. This allows you to hear
145 the difference in variations between the two signals. The annually-averaged values were mapped
146 to pitches between 48 and 96. The monthly-averaged values were mapped to pitches between 60

147 and 108.

148 You can listen to this sonification at

149 https://sdo.gsfc.nasa.gov/iposter/mp3/TS_sunspot_annual_month.mid.mp3



150

151 FIG. 1. Version 2 of the International Sunspot Number as a function of time since 1750. The solid blue line
 152 is the 13-month running average of the values (sampled monthly) and the '+' symbols show the monthly-
 153 averaged values.

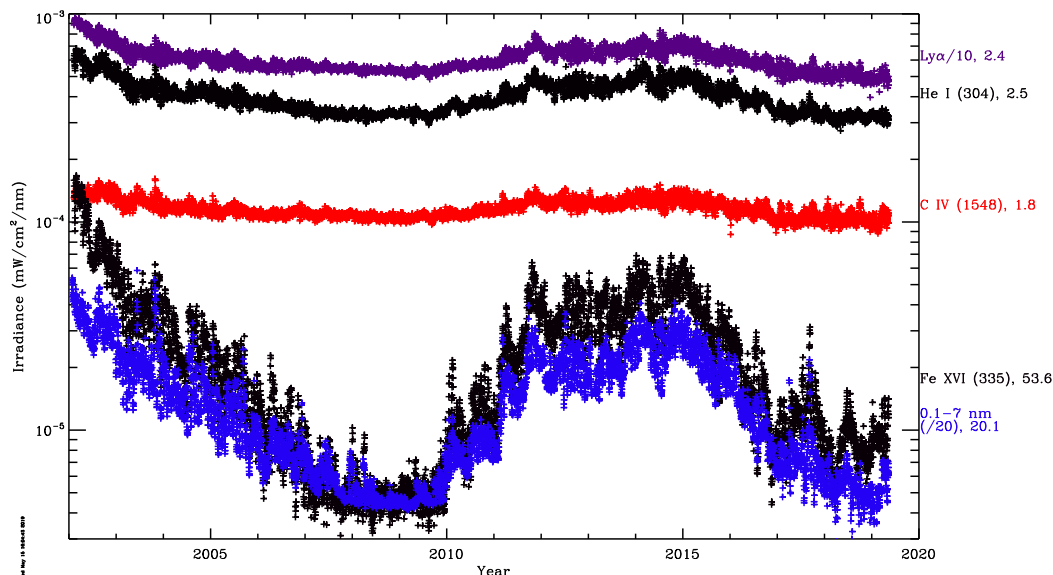
154 B. Extreme Ultraviolet Spectral Irradiances

155 The next example is to sonify extreme ultraviolet (EUV) spectral irradiances from two instru-
 156 ments in two ways. The solar EUV spectral irradiance spans wavelengths between X-rays and
 157 the ultraviolet (roughly 10–100 nm) but is often extended to include the Hydrogen Ly α line at
 158 121.6 nm. This radiation is easily absorbed as it ionizes the outer electrons of many elements.
 159 This also makes it the major source of the ionosphere in the terrestrial and planetary atmospheres.
 160 The EUV emissions are also a direct measure of the magnetic field. The Sun would have consid-
 161 erably smaller EUV emissions if it did not have a magnetic field. For a 6000 K blackbody, the
 162 flux at 30.4 nm is $10^{-26} \times$ the flux at 550 nm. This ratio is 10^{-4} in a solar spectrum. These two
 163 properties, sensitivity to the solar magnetic field and acting as the source of the ionosphere, make
 164 measurements of the solar EUV spectrum a primary goal in solar physics.

165 The longest source of EUV spectral irradiances is the Solar Extreme ultraviolet Experiment⁹

166 on NASA's Thermosphere Ionosphere Mesosphere Energetics and Dynamics (TIMED) spacecraft.
 167 The spectral irradiances from 9 Feb 2002 to 11 May 2019 of several strong lines (He I 304, Ly α
 168 1216, C IV 1548, and Fe XVI 335), along with the 0.1–7 nm radiometer channel, were sonified.
 169 The time dependence of these channels are shown in Figure 2. Pitches between 24 and 108 were
 170 interpolated from the log of the irradiances using the maximum and minimum of each channel
 171 as the limits. This forces the channels to have the same pitch range. The timbres were PIANO,
 172 PICKED_BASS, TROMBONE, FLUTE, and MARIMBA, respectively.

173 You can listen to this sonification at
 174 https://sdo.gsfc.nasa.gov/iposter/mp3/TS_SEE_sonified.mid.mp3



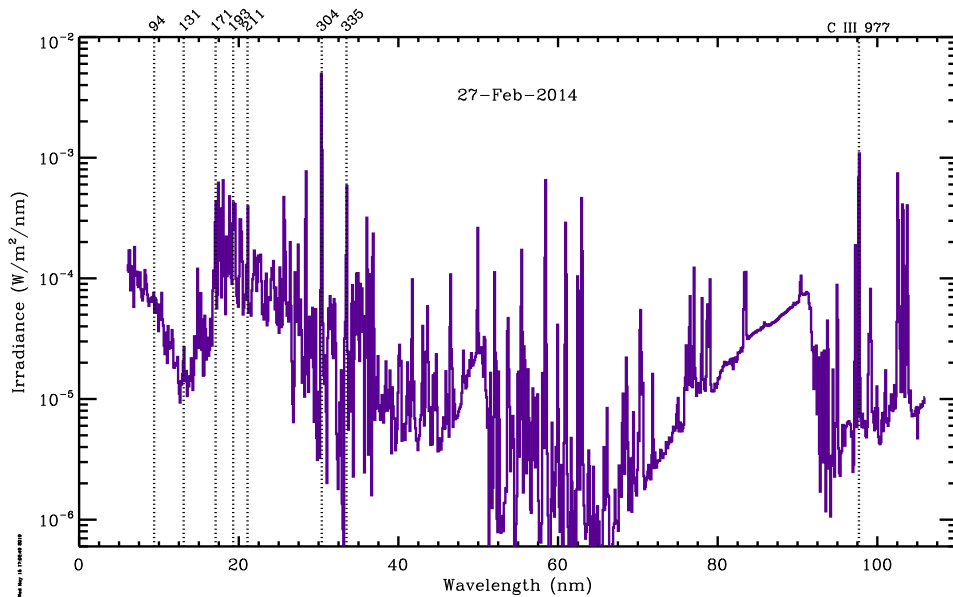
175

176 FIG. 2. EUV spectral irradiances from SEE as a function of time. The selected wavelengths show different
 177 levels of solar cycle modulation. The ratio of the maximum irradiance to the minimum irradiance in each
 178 wavelength is shown as the number after the wavelength identification at right. The Ly α and 0.1–7 nm
 179 irradiances were divided by 10 and 20, respectively, before plotting.

180 EUV spectral irradiances are also available from the Extreme ultraviolet Variability Experiment¹⁰
 181 on NASA's Solar Dynamics Observatory (SDO).¹¹ Data was available from 5 to 105 nm from 1
 182 May 2010 until 26 May 2014 and from 37–105 nm thereafter.

183 Unlike the SEE example, we sonified the solar EUV spectrum from EVE on 2014 Feb 27, the

184 day of maximum sunspot number for Solar Cycle 24 (Figure 3). This shows how the independent



185

186 FIG. 3. A day-averaged EUV spectral irradiance for 22 Feb 2014, as measured by EVE, plotted against the
 187 wavelength in nm. The seven AIA passbands are identified with vertical dashed lines. The He II 304 Å line
 188 is the brightest in this wavelength range, with the C III 977 Å line the next brightest. Although the total
 189 radiant energy in this spectrum is 4.7 mW m^{-2} , about 10^{-5} times the total solar irradiance of 1361 W m^{-2} ,
 190 it is responsible for much of the ionization in the thermospheres of the Earth, Venus, and Mars.

191

192
 193 variable, in this case wavelength, does not have to be time to sonify a data set. The log of the
 194 spectrum irradiances was scaled to MIDI frequencies 36–96. That means every order of magnitude
 195 in the data spans about 1.5 octaves. The PIANO timbre was used. This was the most musical
 196 example. The long progression between 70 and 90 nm resembles parts of the Goldberg Variations.

197 You can listen to this sonification at

198 https://sdo.gsfc.nasa.gov/iposter/mp3/TS_EVE_sonified.mid.mp3

199 C. Extreme Ultraviolet Images

200 Although measuring the EUV spectral irradiance is important, understanding those emissions
 201 requires that you also have images at those wavelengths showing how the source regions of the
 202 emissions vary in both space and time. Extreme ultraviolet images from the Atmospheric Imaging

203 Assembly (AIA)¹² on SDO were sonified as complete images, subimages, and a time sequence of
 204 subimages. AIA provides 10 passbands, seven EUV, two ultraviolet, and one visible light. AIA
 205 193 Å images were selected as they highlighted the desired coronal details. We will describe
 206 different ways to sonify an AIA image from 18 Mar 2018 (20190318_235553_2048_0193.jpg).

207 Images are difficult to sonify because they are dense in information. At a moderate pulse
 208 of 300 bpm, a 512×512 image would take almost 15 hours to complete and a full-resolution
 209 (4096×4096) AIA image would require 40 days. Many people have a hard time remembering
 210 tone sequences and whatever is happening near the end would be disconnected from the begin-
 211 ning. We overcome this by either binning the image to a smaller number of pixels or selecting
 212 subimages. Assuming a person can remember tone sequences for a few minutes, we aim to create
 213 sonifications that last three minutes by binning the image to 32×32 pixels or by using much higher
 214 pulse rates (up to 3000 bpm). Pieces such as John Cage’s *Organ²/ASLSP (As Slow as Possible)*
 215 may be written for performance times of hours to years, but the density of notes is far smaller in
 216 these pieces. According to <https://www.aslsp.org/de/klangwechsel.html>, only 29 notes have been
 217 sounded since a 639 year version of the piece was begun in 2001. An AIA image would sound 29
 218 notes in the first 5.8 s at our standard tempo of 300 bpm.

219 AIA science data is served as monochromatic, 14 bit, files using the Flexible Image Transport
 220 System (FITS).¹³ Quicklook AIA images are served as JPEG files created from the FITS data using
 221 log scaling and an arbitrary color table. There is no information in the separate color channels.
 222 The JPEG images used here were converted to greyscale using the luminosity form to weight the
 223 individual red (R), green (G), and blue (B) channels:

$$IM(B\&W) = 0.21R + 0.72G + 0.07B, \quad (1)$$

224 but starting from the original FITS files would produce very similar results once a logarithmic
 225 scaling was applied. By applying the luminosity form to all JPEG images it is easier to analyze
 226 any image with a three-color format. Images are then sampled along a Hilbert curve as described
 227 above. One initial image is shown in Figure 4, with the left image overdrawn with a raster scan
 228 and the right image overdrawn with a Hilbert curve, which will be described in Section IV below.

229 The image was sampled in two different resolutions. The higher register (pitches 60–120) was
 230 scaled from the 32×32 binned image and assigned the SOPRANO_SAX timbre. The lower
 231 register (pitches 48–96) was scaled from a 16×16 binned image resampled to 32×32 so that both

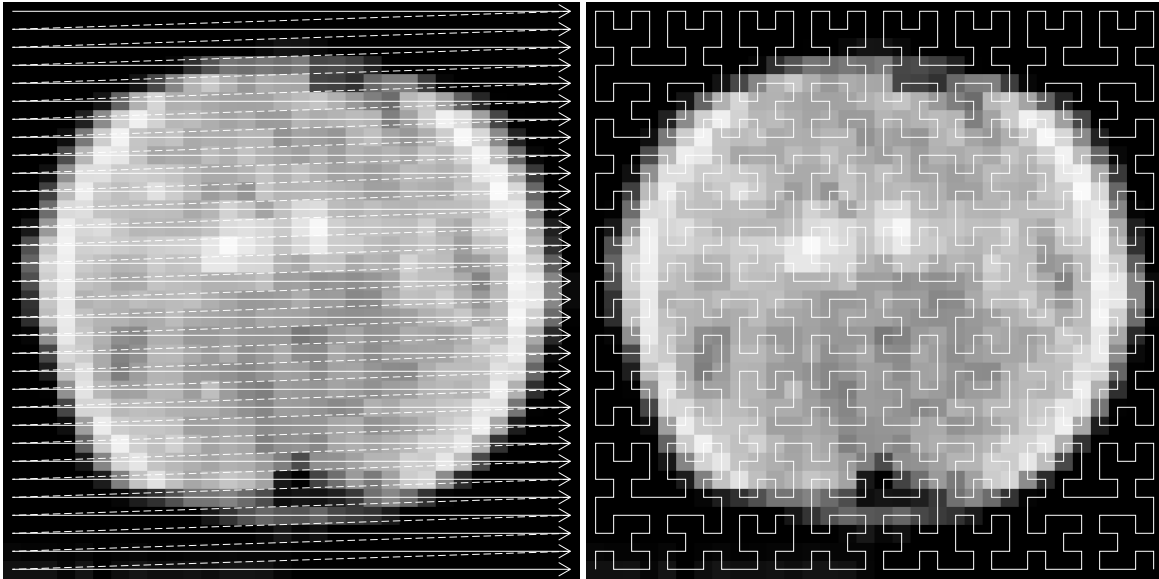


FIG. 4. A greyscale SDO/AIA 193 Å image from 18 Mar 2019 binned from 2048×2048 to 32×32 . On the left is an example of how a raster scan from the top left to the lower right samples the image. The dashed lines are the return from right to left that is not used in the sampling. In the right panel an $n = 5$ Hilbert curve (H_5) is drawn over the image. Each pixel in the image is assigned to a point in the curve. The centers of square pixels are located where the curve has a right angle bend, at the halfway mark of straight segments that are two units long, or two centers proportionally spaced along the straight segments that are three units long.

232 registers have the same number of pulses and assigned the ACOUSTIC_GRAND timbre. The dark
 233 regions of the lower register were omitted by being set to the special variable REST.

234 You can listen to this sonification at

235 https://sdo.gsfc.nasa.gov/iposter/mp3/AIA_193_full_image_sonified_raster.mp3

236 The upper curve (a) in Figure 5 shows how the raster scan is dominated by the quasi-periodic
 237 variations caused by the scan moving onto and off of the disk of the Sun. As a result, we explored
 238 using other methods to sample the image. The Hilbert curve was one of those methods.

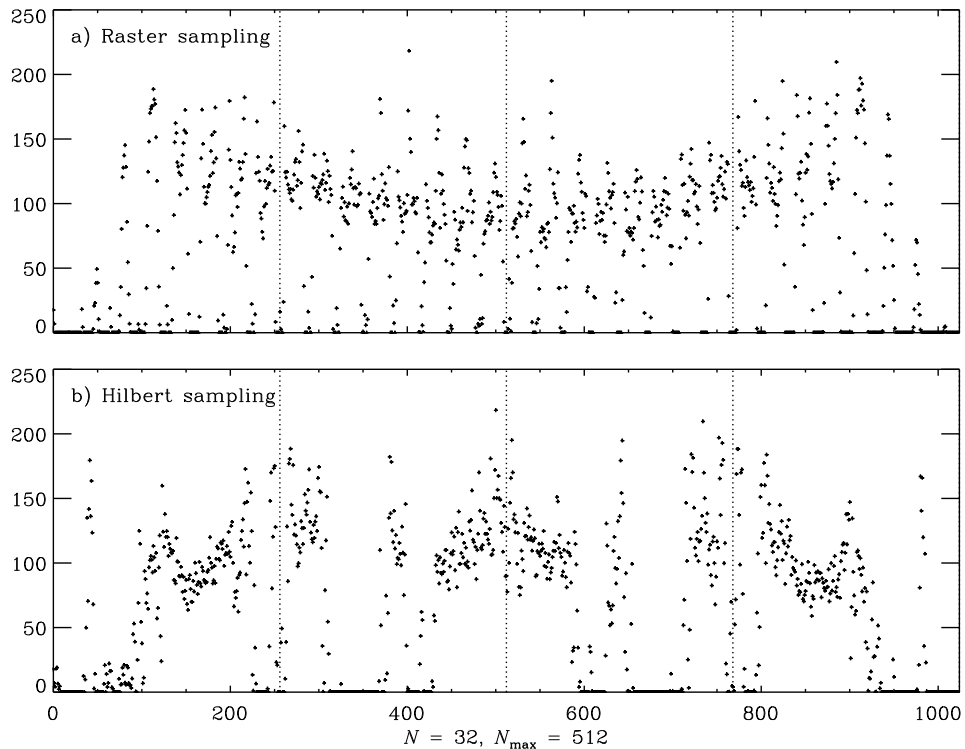


FIG. 5. Sampling curves for the AIA 193 Å image in Figure 4 binned to 32×32 . The top plot (a) used a raster scan to sample the pixels (the left panel in Figure 4.) The lower plot (b) used a Hilbert curve to address the image (the left panel in Figure 4.) The vertical lines show the four horizontal strips of (a) and the quadrants of (b).

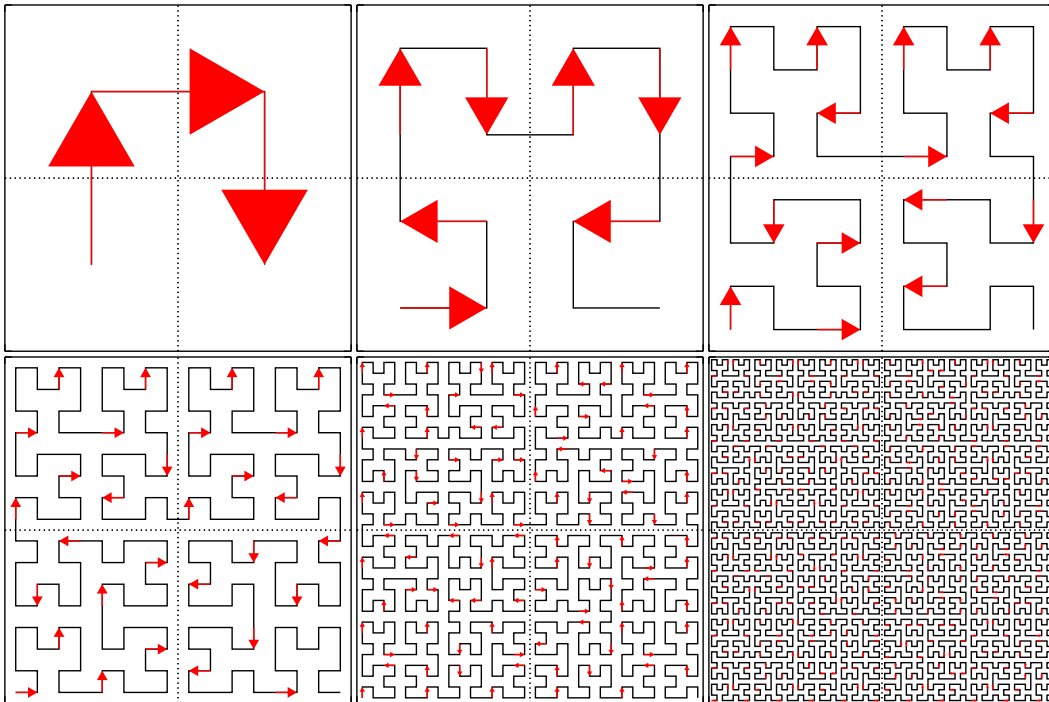
239 IV. HILBERT CURVES

240 Hilbert curves are continuous space-filling curves that have been used in a surprisingly large
 241 number of disciplines. They were first described by Hilbert¹⁴ as a simpler form of the space-filling
 242 curves of Peano¹⁵. A true Hilbert curve exists only as the limit of $n \rightarrow \infty$ of the n^{th} approximation
 243 to a Hilbert curve (H_n). However, the approximations are useful to provide mappings of 2-D
 244 images onto a 1-D sequence. Figure 6 shows H_n for $n = 1, 2, \dots, 6$.

245 A summary of properties of H_n :

- 246 1. There are 2^n pixels along each side of the square containing the curve
- 247 2. The Euclidean length of H_n grows exponentially with n , $2^n - 2^{-n}$

- 248 3. H_n covers a finite area as it is always bounded by the unit square
- 249 4. Two points in the image, (x_1, y_2) and (x_2, y_2) , that are close together in H_n are also, with a
- 250 few exceptions, close together in $H_{n'}$, $n' > n$



251

252 FIG. 6. The first six Hilbert curves, plotted from upper left to lower right, with arrows showing the direction

253 of the motion into each vertex. Each subplot is drawn with axes limits of $[0,1]$ in both directions. Among

254 the most important properties of these curves is the single line connecting two quadrants. This can be seen

255 by examining the dotted lines drawn to separate the quadrants. Another property is that the sampling goes

256 around each quadrant in a similar motion (upper quadrants are sampled in a clockwise fashion and the lower

257 quadrants in a counter-clockwise fashion.

258 A Hilbert curve maps a linear variable onto the two-dimensional coordinates of an image. Its

259 inverse is a mapping of the image coordinates onto a linear variable. This mapping property means

260 we can use Hilbert curves to map solar images onto a linear sequence of pixel values that can then

261 be sonified. Images tend to have dimensions that are powers of 2, so the Hilbert curves are a natural

262 fit to addressing them.

263 Reading the image along a Hilbert curve has the advantage of keeping neighborhoods close to-
 264 gether as the resolution (i.e., the length of the curve) increases. It also removes most of the detec-
 265 tor size periodicities and actually shows the presence of longer-scale features. Because successive
 266 H_n 's pass through similar neighborhoods as the resolution is refined, Hilbert curve samplings can
 267 be overplotted in time to provide contrasting versions of the image.

268 The neighborhood property works with other space-filling curves. Bartholdi et al.¹⁶ describe
 269 using a Sierpinski space-filling curve to design delivery routes for Meals on Wheels. The system
 270 was simple, cheap, and paper-based. It used a manual "Rolodex" method of entering or removing
 271 addresses.

272 Vinoy et al.¹⁷ and others have shown how to use Hilbert curves to construct microwave an-
 273 tennas. They used models and measurements of the input impedance to show that a small square
 274 overlain with a conducting Hilbert curve produced an antenna whose resonance frequencies were
 275 consistent with a much longer wire antenna. They also showed how those frequencies shifted and
 276 how additional resonances were added as the order of the Hilbert curve was increased. This makes
 277 these antennas useful for mobile wireless devices.

278 Seeger and Widmayer¹⁸ describe using space-filling curves to access multi-dimensional datasets
 279 with a 1-D addressing scheme. The 1-D curve imposes an order on the data access that is difficult
 280 to implement using a multi-dimensional access polynomial.

281 Multi-dimensional Fourier integrals (as well as others) can be reduced to a 1-D form by map-
 282 ping the coordinates onto a space-filling curve, essentially converting the integral into a Lebesgue
 283 integral.¹⁹

284 V. EXTREME ULTRAVIOLET IMAGES SAMPLED ALONG HILBERT CURVES

285 The difference between the sampling along a Hilbert curve and a raster scan can be seen in
 286 Figure 5, where the sampling curves for the image in Figure 4 (binned to 32×32) are shown. The
 287 bottom curve (b) in Figure 5 shows how the Hilbert curve sampling localizes the off-disk portions
 288 of the image along the curve and hence in time in the sonified version.

289 The pixels in the raster scan sonification were converted to tones by mapping pixels values
 290 between [0,250] to pitches [60, 120] (or C4 to C9, a span of 5 octaves). The duration was set to a

291 sixteenth note, the loudness to 110, and the PIANO timbre was used. In the Hilbert curve sampling
292 the full-resolution pixels were sonified with the same values except the SOPRANO_SAX timbre
293 was used. A second voice was added mapping pixels values between [0,250] to pitches [48, 96]
294 (or C3 to C7, a span of 4 octaves). The duration was set to a quarter note, the loudness to 90, and
295 the ACOUSTIC_GRAND timbre was used.

296 You can listen to this sonification at
297 https://sdo.gsfc.nasa.gov/iposter/mp3/whole_AIA_193_full_image_sonified.mid.mp3

298 **A. Using Subimages to Emphasize Features in Extreme Ultraviolet Images**

299 The AIA 193 Å image in Figure 5 is vastly undersampled. The length of an image sonification
300 scales as n^2 , where n is the order of the Hilbert curve. One way to increase the accuracy of the
301 sampling while keeping a reasonable length in the sonification is to sub-sample the image. Seven
302 64×64 subimages of the 2019 Mar 18 image are shown in Figure 7, numbered to agree with
303 Table I.

304 The duration was set to a sixteenth note, the loudness to 110, and the PIANO timbre was used.
305 Each subimage was sampled along a Hilbert curve. The full-resolution pixels were sonified with
306 the same values as the full image Hilbert curve sampling example above with the exception that
307 the range of pixel values was [0, 255]. A second voice was added mapping pixels values between
308 [0,255] to pitches [48, 84] (or C3 to C6, a span of 3 octaves). The duration was set to a quarter
309 note, the loudness to 75, and the ACOUSTIC_GRAND timbre was used.

310 You can listen to this sonifications by accessing the clickable image at
311 <https://sdo.gsfc.nasa.gov/iposter/>.

313 **B. Filament Liftoff Sequence in Extreme Ultraviolet Images**

314 The final example is sonifying a series of images from AIA on SDO. We selected the filament
315 liftoff of 2010 Mar 10–12 as the first example. Eight subimages were extracted that included the
316 filament liftoff and the first two quadrants of those subimages were sampled along a Hilbert curve
317 and sonified. A short chorus and ending cadence were written. The piece was made by inserting
318 the subimages in turn, separated by a chorus and ending with the cadence, thus creating a single

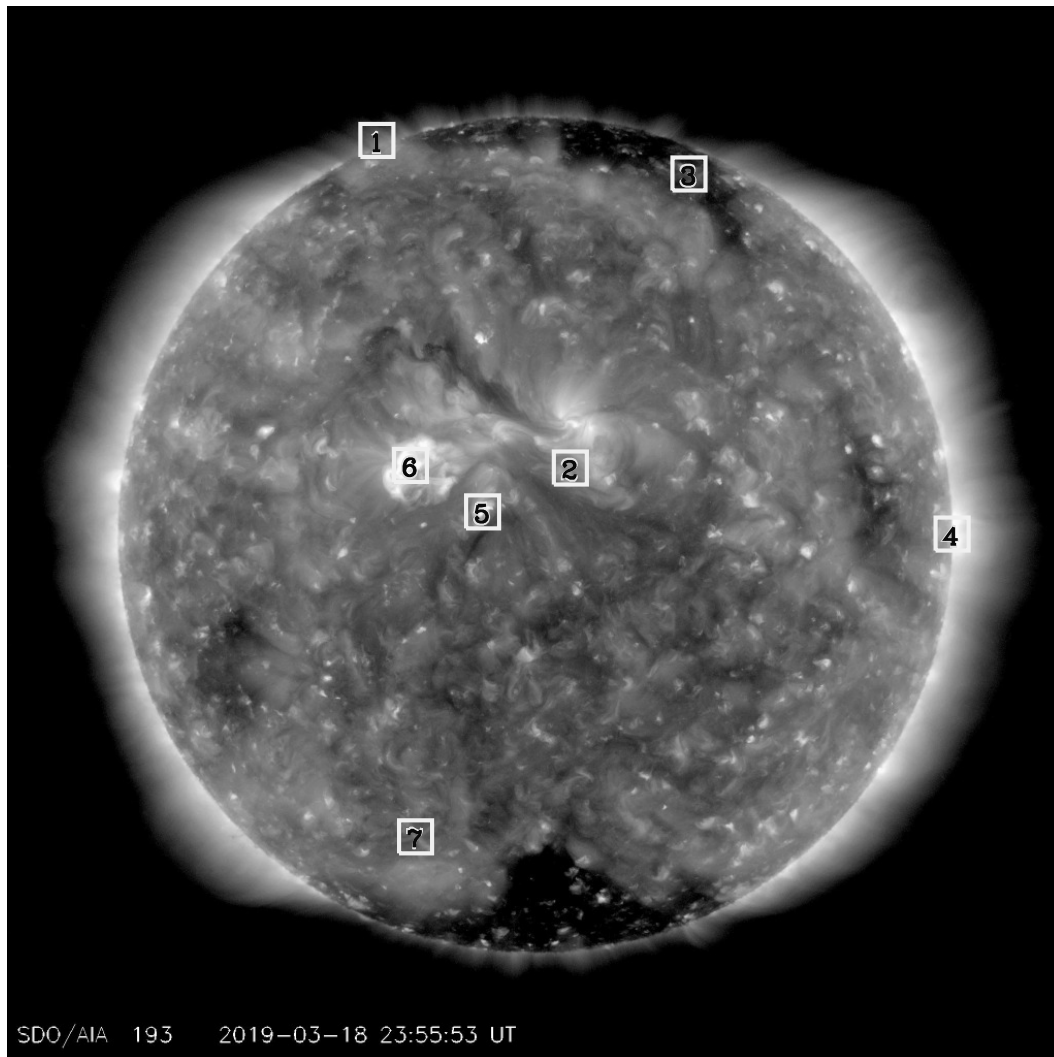


FIG. 7. A greyscale SDO/AIA 193 Å image from 18 Mar 2019. This image will be used as an example for sonifying still images. The boxes mark the locations of the examples in Table I.

319 time series of pitches.

320 The pixels in this sequence were converted to tones by mapping $[-60, 60]$ to pitches $[36, 96]$ (or
 321 C2 to C7, a span of 5 octaves). The duration was set to a sixteenth note, the loudness to 110, and
 322 the PIANO timbre was used.

323 You can listen to this sonification at

324 https://sdo.gsfc.nasa.gov/iposter/mp3/liftoff_complete.mid.mp3

325 This was the least satisfying sonification because the changes in time were subtle and difficult

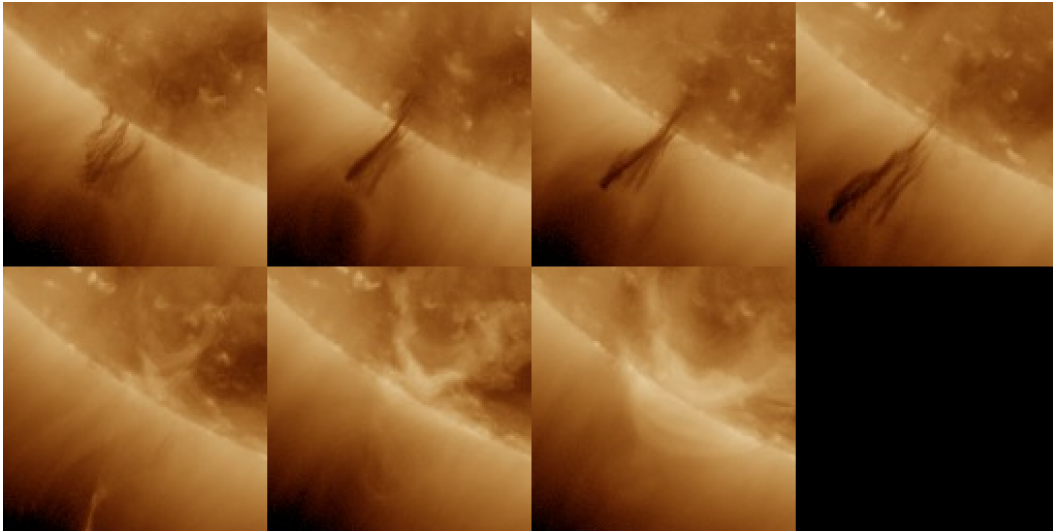


FIG. 8. Montage of seven solar images showing a filament liftoff.

326 to resolve. We have been investigating other ways to show the movement of material through both
 327 space and time.

328 VI. DISCUSSION OF SONIFIED DATA

329 Based on our experiments, percussive sounds, such as PIANO and PICKED_BASS, seem to
 330 work better for sonifying data. Percussive timbres securely place the sound on the beat and produce
 331 interesting changes as the tempo increases. A timbre with a noticeable rise or decay time tends to
 332 sound muddy as the tempo is increased.

333 Our attempts to create a beat and melody by playing two versions of averaged data, such as the
 334 annual vs. the monthly values of S , were not a complete success. We continue to explore how to
 335 make the sonified data more like music and less mechanical.

336 Although sonified data does not sound like most types of music, at least one piece of classical
 337 music has similar qualities. Bach's Goldberg Variations (BWV 988) sounds much like the image
 338 sonifications described above. One part, at around the 33-minute mark as played by Glenn Gould
 339 in his 1955 debut album of the same name, has a long chromatic run that sounds like one part of the
 340 EUV spectrum. The rapid increases in pitch of the strong spectral lines also add musical contrast
 341 to the piece.

342 You cannot create an MP3 file directly from the JythonMusic synthesizer. You can capture the
343 sounds in a recorder as the MIDI commands are executed. Or you can load the file containing the
344 commands into another synthesizer. The MP3 files listed here were created by playing the MIDI
345 files in GarageBand, a proprietary program from Apple. You can also easily change the timbre of
346 a part in GarageBand, providing another level of experimentation. Different synthesizers assign
347 different timbres to each instrument channel, so the listed MP3 files do not always match what
348 is heard when the JythonMusic synthesizer is used. Other timbre files can also be used with the
349 synthesizers.

350 You can also use other programs to generate the MIDI file from a dataset. For example,
351 Lilypond²⁰ is a music engraving program that can also produce a MIDI file that is playable in
352 GarageBand or other synthesizer. You also get a beautiful score of the piece as a bonus. Similar
353 to the JythonMusic workflow, the data file was opened in IDL, the data was scaled to pitches and
354 those pitches were written in Lilypond syntax to a Lilypond-readable file. An example of a score
355 is shown in Figure 9. Strong spectral lines can be seen in measures 31 and 35.

357 Mapping data to variations in pitch may not be the optimum solution for sonifying data. A large
358 value of a dataset may be better represented by changes in the volume, emphasizing the strength of
359 the larger value. We did some experiments on such variations and found that the limited ability of
360 humans to sense changes in loudness and to remember a baseline level of loudness over an entire
361 piece made this less effective at sonifying data. Sonifying the data using a constant pitch with
362 variable loudness also led to annoyance caused by the unchanging pitch.

363 Other examples of sonifying solar data include solar oscillations,^{21,22} solar wind data,²³ and an
364 interactive image to music experience.²⁴ The first three examples are for 1-D time series while the
365 fourth uses the motion of a person to sample an image. Others have produced a sonified solar
366 system.²⁵ The image sonifications described herein may be one of the few examples of such a
367 project.

368 VII. CONCLUSIONS

369 We have sonified solar data as time series, two versions of the EUV spectral irradiance, EUV
370 images with various techniques, and a time sequence of EUV images. The EUV spectrum showed

EUV on 27 Feb 2014 (Solar Maximum)

Piano Old Sol

FIG. 9. The first page of a piano score of the EVE spectrum in Figure 3 created by Lilypond. The He II 304 Å line can be seen in measure 31 and the Fe XVI 335 Å line in measure 35. The scaling to pitch is different than the sonified example to better fit on the staves.

371 that the independent variable does not have to be time. We demonstrated that using a Hilbert curve
 372 to address a solar image gives a sonification that shows more of the image variations and less of
 373 the shape of the Sun.

374 One shortcoming of the Hilbert curve sampling method is the separation of two regions near the
 375 limb. In these examples, images are sampled by a curve that crosses from the upper left quadrant
 376 to the upper right near the equator. This means the northern polar region is sampled in two distinct
 377 areas far from one another. The two lower quadrants do not have a direct connection and the
 378 southern polar region is also divided into two distinct regions, one at the beginning of the series
 379 and the other at the end. This can be remedied by rotating the Hilbert curve (or the image) 90°
 380 in either direction, which moves the connection between quadrants to the poles and keeps those
 381 regions in a smaller neighborhood while dividing the equatorial limb sectors into disparate parts of

382 the sampling curve.

383 Other techniques can be used to sonify solar images. Coincident images observed in different
384 wavelengths of light can be sampled and placed in different timbres or pan positions. Once the next
385 solar maximum passes another EVE spectrum could be used to play against the solar maximum
386 spectrum illustrated here. Higher-order Hilbert curves can be constructed to sample a series of
387 images. This would keep points within a neighborhood in both space and time.

388 Sonifying solar images is a way to explore the interface between tempo and pitch. Increasing
389 the tempo to 3000 bpm (or 50 Hz) allows you to investigate whether an extremely rapid tempo
390 results in an envelope with the individual pitches providing an amplitude modulation of that enve-
391 lope. Frequencies of 15–30 Hz (900–1800 bpm) are near the limit of pitch discrimination.²⁶ The
392 difference between the buzz saw of the raster scan image (Sec. III C) and the smoother sound of
393 Hilbert curve sampling of Sec. V is one example of how the envelope makes a big difference in the
394 perception of the data.

395 Listening to the Sun allows people to enjoy our closest star in a new direction. This does not
396 apply only to the blind, most people can hear the variations of the Sun. With time these techniques
397 will also allow people to more fully explore images as well.

398 VIII. QUESTIONS AND OTHER PROJECTS

399 Here are some ideas that can motivate students to listen to their data:

- 400 1. Can you find ways to vary the pulse of the music? Scientific data tends to have even spac-
401 ing and the simplest way to sonify the data is to maintain an even pulse. You can use the
402 JythonMusic routine `Mod.tie.Pitches` to tie together identical notes to add some variety to
403 the rhythmic spacing. Another routine, `Mod.accent` allows you to accent a beat, which also
404 provides some texture to the music.
- 405 2. There are 3-color AIA images that can be sonified by assigning a voice and pan position to
406 each of the channels that will emphasize the differences in the channels.
- 407 3. A wavelet analysis of a time series can be used to isolate persistent from ephemeral frequen-
408 cies. Can a wavelet spectrum be sonified to show the persistent frequencies as droning notes

409 and ephemeral events as more rapid variations?

- 410 4. Can other instruments be played against the synthesizer output? The sonified data has no
411 explicit key, so improvised solos and rhythms can be played along with the sonified data.

412 ACKNOWLEDGMENTS

413 This work was supported by NASA's Solar Dynamics Observatory at the Goddard Space Flight
414 Center. KIG participated in this research as part of the requirements for his Research Practicum at
415 Eleanor Roosevelt High School. He would like to acknowledge the assistance and support of Ms.
416 Yau-Jong Twu. WDP would like to thank Prof. Hofstetter for an introduction to electronic music.
417 Version 4.6 of the JythonMusic software was downloaded from <https://jythonmusic.me>. All of the
418 data used in this research is available as continually updated files from publicly-accessible sites.
419 The monthly averaged (SN_m_tot_V2.0.csv) and the annually averaged (SN_y_tot_V2.0.csv) In-
420 ternational Sunspot Number (Version 2) data were obtained from the Solar Influences Data Cen-
421 ter (<http://sidc.oma.be/silso/datafiles>). Daily averaged SEE measurements were obtained as the
422 SEE Level 3 Merged NetCDF file at http://lasp.colorado.edu/data/timed_see/level3/latest_
423 [see_L3_merged.ncdf](http://lasp.colorado.edu/data/timed_see/level3/latest_see_L3_merged.ncdf). Daily averaged EVE measurements were obtained the EVE Level 3 Merged
424 NetCDF file at http://lasp.colorado.edu/eve/data_access/evewebdataproducts/merged/EVE_
425 [L3_merged_1a_2019135_006.ncdf](http://lasp.colorado.edu/eve/data_access/evewebdataproducts/merged/EVE_L3_merged_1a_2019135_006.ncdf). AIA images were obtained as JPEGs from the SDO website
426 <https://SDO.gsfc.nasa.gov>.

427 * William.D.Pesnell@NASA.gov

428 ¹ Dieter Daniels. Luigi russolo «intonarumori», 2020. URL [http://www.medienkunstnetz.de/works/
429 intonarumori/audio/1/](http://www.medienkunstnetz.de/works/intonarumori/audio/1/).

430 ² Iannis Xenakis. Electro-acoustic music. Vinyl LP, Nonesuch H-71246, 1970.

431 ³ John H. Flowers. Thirteen years of reflection on auditory graphing: Promises, pitfalls, and potential new
432 directions. In *Proceedings of ICAD 05-Eleventh Meeting of the International Conference on Auditory
433 Display, Limerick, Ireland, July 6-9, 2005*, pages 406–409, 2005.

- 434 ⁴ G. M. Morton. A computer oriented geodetic data base; and a new technique in file sequencing. Technical
435 report, IBM Ltd., Ottawa, Canada, 1966.
- 436 ⁵ Bill Manaris and Andrew R. Brown. *Making Music with Computers: Creative Programming in Python*.
437 Taylor and Francis Group, LLC, Boca Raton, Florida, 2014.
- 438 ⁶ John Backus. *The Acoustical Foundations of Music*. W. W. Norton & Company, New York, 1969. This
439 work has been revised and updated in ISO 226:2003 but the conclusions needed here remain valid.
- 440 ⁷ F. Clette, L. Svalgaard, J. M. Vaquero, and E. W. Cliver. Revisiting the Sunspot Number. A 400-Year
441 Perspective on the Solar Cycle. *Space Sci. Rev.*, 186:35–103, December 2014. doi:10.1007/s11214-014-
442 0074-2.
- 443 ⁸ Frédéric Clette and Laure Lefèvre. The new sunspot number: Assembling all corrections. *Solar Phys.*,
444 291:2629–2651, 2016. doi:10.1007/s11207-016-1014-y.
- 445 ⁹ T. Woods, S. Bailey, F. Eparvier, G. Lawrence, J. Lean, B. McClintock, R. Roble, G. Rottman,
446 S. Solomon, and W. Tobiska. TIMED Solar EUV experiment. *Physics and Chemistry of the Earth*
447 *C*, 25:393–396, 2000. doi:10.1016/S1464-1917(00)00040-4.
- 448 ¹⁰ T. N. Woods, F. G. Eparvier, R. Hock, A. R. Jones, D. Woodraska, D. Judge, L. Didkovsky, J. Lean,
449 J. Mariska, H. Warren, D. McMullin, P. Chamberlin, G. Berthiaume, S. Bailey, T. Fuller-Rowell, J. Sojka,
450 W. K. Tobiska, and R. Viereck. Extreme Ultraviolet Variability Experiment (EVE) on the Solar Dynamics
451 Observatory (SDO): Overview of Science Objectives, Instrument Design, Data Products, and Model
452 Developments. *Solar Phys.*, 275:115–143, January 2012. doi:10.1007/s11207-009-9487-6.
- 453 ¹¹ W. D. Pesnell, B. J. Thompson, and P. C. Chamberlin. The Solar Dynamics Observatory (SDO). *Solar*
454 *Phys.*, 275:3–15, January 2012. doi:10.1007/s11207-011-9841-3.
- 455 ¹² J. R. Lemen, A. M. Title, D. J. Akin, P. F. Boerner, C. Chou, J. F. Drake, D. W. Duncan, C. G. Edwards,
456 F. M. Friedlaender, G. F. Heyman, N. E. Hurlburt, N. L. Katz, G. D. Kushner, M. Levay, R. W. Lindgren,
457 D. P. Mathur, E. L. McFeaters, S. Mitchell, R. A. Rehse, C. J. Schrijver, L. A. Springer, R. A. Stern,
458 T. D. Tarbell, J.-P. Wuelser, C. J. Wolfson, C. Yanari, J. A. Bookbinder, P. N. Cheimets, D. Caldwell,
459 E. E. Deluca, R. Gates, L. Golub, S. Park, W. A. Podgorski, R. I. Bush, P. H. Scherrer, M. A. Gummin,
460 P. Smith, G. Auken, P. Jerram, P. Pool, R. Soufli, D. L. Windt, S. Beardsley, M. Clapp, J. Lang, and
461 N. Waltham. The Atmospheric Imaging Assembly (AIA) on the Solar Dynamics Observatory (SDO).
462 *Solar Phys.*, 275:17–40, January 2012. doi:10.1007/s11207-011-9776-8.

- 463 ¹³ W. D. Pence, L. Chiappetti, C. G. Page, R. A. Shaw, and E. Stobie. Definition of the Flexible Im-
464 age Transport System (FITS), version 3.0. *A. & Ap.*, 524:A42, December 2010. doi:10.1051/0004-
465 6361/201015362.
- 466 ¹⁴ D. Hilbert. Über die stetige abbildung einer linie auf ein flächenstück. *Mathematische Annalen*, 38:
467 459–460, 1891.
- 468 ¹⁵ G. Peano. Sur une courbe, qui remplit toute une aire plane. *Mathematische Annalen*, 36:157–160, 1890.
- 469 ¹⁶ John J. Bartholdi, Loren K. Platzman, R. Lee Collins, and William H. Warden. A minimal technology
470 routing system for Meals on Wheels. *Interfaces*, 13(3):1–8, 1983.
- 471 ¹⁷ K. J. Vinoy, K. A. Jose, V. K. Varadan, and V. V. Varadan. Hilbert curve fractal antenna: A small resonant
472 antenna for VHF/UHF applications. *Microwave Opt Technol Lett*, 29(4):215–219, 2001.
- 473 ¹⁸ Bernhard Seeger and Peter Widmayer. Geographic information systems. In Sartaj Sahni and Dinesh P.
474 Mehta, editors, *Handbook of Data Structures and Applications*, chapter 56. CRC Press, Boca Raton,
475 Florida, 2nd edition, 2018.
- 476 ¹⁹ Norbert Wiener. *The Fourier Integral and Certain of its Applications*. Dover, New York, 1933.
- 477 ²⁰ Lilypond. Lilypond . . . music notation for everyone, 2020. URL <http://lilypond.org>.
- 478 ²¹ Alexander G. Kosovichev. Solar Sounds, 1997. URL <http://soi.stanford.edu/results/sounds.html>.
- 479 ²² Tim Larson. SoSH Project: Sonification of Solar Harmonics, 2020. URL <http://solar-center.stanford.edu/sosh/>.
- 481 ²³ Andrea effe Rao. Sounds from the Sun - Data Sonification - Thesis, 2016. URL <https://www.behance.net/gallery/35831845/Sounds-from-the-Sun-Data-Sonification-Thesis>.
- 483 ²⁴ Marty Quinn. “Walk on the Sun”: An interactive image sonification exhibit. *AI & SOCIETY*, 27(2):
484 303–305, 2012. doi:10.1007/s00146-011-0355-1. URL <https://doi.org/10.1007/s00146-011-0355-1>.
- 485 ²⁵ Michael Quinton, Iain McGregor, and David Benyon. Sonifying the solar system. In *The 22nd Interna-*
486 *tional Conference on Auditory Display (ICAD-2016)*, pages 28–35, 07 2016. doi:10.21785/icad2016.003.
- 487 ²⁶ John Backus. *The Acoustical Foundations of Music*. W. W. Norton & Company, New York, 1969. Ch. 7.